APPLICANT'S EXHIBIT 57

Paper No.
24

CORROSION 96
The NACE International Annual Conference and Exposition

CORROSION MANAGEMENT IN THE ARUN FIELD

L. M. Riekels, R. V. Seetharam, R. M. Krishnamurthy, C. F. Kroen, J. L. Pacheco,
R. H. Hausler, and V. A. W. Semerad
Mobil Oil Corporation
13777 Midway Road
Farmers Branch, TX 75244-4312

N. Kaczorowski
Mobil Oil Indonesia, Inc.
P.O. Box 61, Lhok Seumawe
North Aceh Province, Sumatra, Indonesia

ABSTRACT

A risk model has been developed to identify the probability that unacceptable downhole corrosion would occur as the Arun field was depleted. Using the life expectancy estimates for the carbon steel tubing strings from this model, optimized mitigation strategies could be developed to provide cost-effective alternatives for the management of corrosion.

Keywords: localized corrosion, downhole corrosion, condensate inhibition, corrosion risk model, extreme value statistics, Arun corrosion, life expectancy

INTRODUCTION

The Arun field, located on the northern coast of the Aceh province in North Sumatra, Indonesia, is a gas condensate reservoir that was discovered in 1971 and has been in production since 1977. The reservoir is a compositionally dynamic system where retrograde condensation, condensate revaporization, water vaporization, mixing of lean injection gas, gas dehydration, and booster compression impact reservoir performance. In order to manage corrosion and its potential impact on gas deliverability, it was necessary to assess the probability that unacceptable downhole corrosion would occur as the Arun field was depleted. The changes in the wellbore environment over time which could influence corrosion kinetics had to be identified. Reservoir model data were used as inputs for a compositional tubing hydraulics program. This program generated pressure-temperature profiles in the wellbores as a function of depth, liquid dropout volumes for water and hydrocarbon phases, and the properties of the liquid films that develop during annular two-phase flow. Using multi-parameter regression analysis, results from field workover inspections, and laboratory corrosion testing, a corrosion risk model was developed to provide estimates of the life expectancy for the existing tubing in the Arun wellbores. Optimized mitigation strategies could then be developed to provide cost-effective alternatives for the management of corrosion.

PREVIOUS WORK

A significant effort[1,2,3,4,5,6,7] has been expended in the evaluation of the probability for downhole corrosion as the field is depleted. The complexity of the downhole environmental systems and the potential synergy between the variables in these systems has presented a continuing challenge to those attempting to interpret dynamic corrosion behavior throughout the life of the reservoir. Predictions of the probability for unacceptable corrosion of the L80 tubing string completions in the Arun wellbores is complicated by the interactive variables in the environment, including wellstream composition, reservoir pressure, flow regime-pressure-temperature profiles in the tubing string, condensate quality and wetting characteristics, tubing metallurgy, shear stress, and water condensation and composition.

It has been known that with pressure depletion of the reservoir, substantial water vaporization would occur, resulting in an exponential increase in the water vapor fraction. No movement of the gas/water contact in the reservoir was anticipated so all liquid water production would be due to the condensation of water vapor. Due to the high production rates, the Arun wells have been in an annular mist flow regime with the majority of the liquid entrained in droplets in the flowing gas stream. As the pressure declines, less liquid hydrocarbon and more water is produced and the produced gas becomes leaner due to the reinjection of separator gas. The injected gas changes the composition of the reservoir gas and lowers the dew point pressure of the mixture.

In most condensate wells, the hydrocarbon condensate is produced along with a small amount of condensed water. However, if the water condenses in the production tubing string before the hydrocarbon condensate is formed, a corrosive condition may exist. When the tubing walls become wet with CO_2 saturated water, it is known that the corrosion rate can increase dramatically. Corrosion would be expected to be proportional to the time fraction that the metal is wetted on a microscopic scale by the aqueous phase. No corrosion would take place if the hydrocarbon is a continuous phase on the steel surface. Impingement of water droplets on the steel surface will, in effect, increase the amount of water exposure even if the oil phase is continuous on the steel surface. Thus, high flow rates can contribute to the water wetting and corrosion.[8]

Liquid Volume Ratio of Water and Hydrocarbon

Some rules of thumb[9] have been developed regarding the water production rates and the wetting of steel surfaces. The interfacial properties of the liquids, both water and hydrocarbon, with steel will determine which species will preferentially wet the surface. Research[10] has indicated that the nature of the oil itself will affect these wetting tendencies.

Using the rules of thumb from field experience and the similarities between the Arun condensate and other condensates which have been studied, it was suspected that the Arun condensate may naturally inhibit corrosion under certain producing conditions. Based on field experience and experimental work with condensates reported in the literature, it was hypothesized that the volume ratio of liquid water to liquid hydrocarbon greater than about 0.5 (one-third water and two-thirds condensate) would be likely to result in corrosion, which could vary from mild to severe depending on the corrosivity of the acidic water.

Both liquid water and liquid condensate will condense out in a tubing string when their respective dew points have been reached. In a preliminary analysis with an initial version of a reservoir simulation model for the Arun field and a downhole tubing hydraulics program,[1] the liquid volumes for both water and hydrocarbon phases were estimated in one tubing string over time as the reservoir was depleted. Figure 1 shows the profiles of the volume ratio of liquid water to liquid hydrocarbon vs. the tubing temperature from bottomhole to the top of the tubing string. The increase in the volume ratio with time is evident. A zone of high probability corrosion damage was estimated with boundaries as the temperature range from 225 to 275°F (107 to 135°C), where previous work[3] had shown maximum susceptibility to localized corrosion, and a minimum value of 0.5 for the volume ratio of water to hydrocarbon. With this preliminary prediction, it was estimated that serious wellbore corrosion problems could be encountered at the top of this tubing string by the year 2000.

In order to attempt to identify possible alternatives to manage the occurrence of unacceptable corrosion, an interdisciplinary team then began to further refine the assumptions and to verify the hypothesized parameter ranges for corrosion damage for all 78 producing wells.

Reservoir Management Data

The downhole environment in Arun wellbores is the result of the complex interaction between thermodynamic and flow phenomena:

- As the Arun fluid undergoes retrograde condensation, liquid drops out in the reservoir and reduces well productivity. This changes inflow conditions such as bottomhole pressures and well production rates.
- As the reservoir depletes, and as injected gas breaks through, the composition of the fluid entering the wellstream changes.
- The temperature profile along the tubing string is determined by the type of completion fluid used, well rate, and wellstream compositions.
- Changes in the temperature and pressure along the tubing string result in hydrocarbon liquid dropout. The extent of such dropout increases initially as the pressure drops (retrograde condensation), then decreases as the pressure drops further (revaporization). The liquid volume also increases at cooler temperatures and varies with the fluid composition.
- The water vapor content of the wellstream increases rapidly as the reservoir pressure depletes. This water then condenses on the tubing string increasingly as it reaches lower temperatures and pressures.
- When the well rate drops below a critical point, the gas phase is unable to carry the entrained liquid and the well shuts down due to liquid loading.

All of these phenomena and their interaction were modeled using a compositional tubing hydraulics program. This program solves the thermodynamic, momentum, and energy equations to fully capture the above effects. It has been validated against field measured pressure traverses which have shown that the model predictions agree well with field data over a wide range of conditions.

In the reservoir, single phase flow is assumed, with liquid dropout effects captured in the form of an effective permeability. A simple pseudo-gas potential (m(p)) equation is used for this single-phase gas inflow, including non-Darcy effects. The wellbore calculations, however, are fully compositional and involve multiple phases. A correlation was developed for the Arun field, relating field-measured condensate-to-gas ratios (CGRs) and separator temperatures to the composition of the wellbore gas. This correlation, which accounts for compositional changes due to pressure depletion and mixing with injected lean gas, was verified against simulation results and a limited number of field composition measurements. The Peng-Robinson equation of state (EOS)[18] is used to model the thermodynamic equilibrium assumed prevalent in each of the tubing segments and a 9-component fluid model is used to represent the Arun gas condensate. The amount and compositions of each of the three phases (wellstream gas, liquid hydrocarbon, and liquid water) in each segment are determined by solving the thermodynamic equations.

Energy balance equations are used to model heat loss from the wellstream to the surroundings and the resulting temperature profile in the tubing string. The modified Gray correlation[19] for multi-phase flow is used to predict pressure drops in the segments, based on amount of liquid present, diameter and roughness of the segments, and properties of the various phases present. The compositional tubing hydraulics program can determine the tubing head pressure (THP) at a given well rate, or alternatively, predict the well rate at a given THP.

The downhole environment parameters for each of the 78 Arun wells were generated over the past producing life (history phase) and over the projected flowing life (prediction phase). In the history phase, field data sources such as the production database, buildup and shut-in pressure surveys, fluid analyses, and well diagrams were used to extract input data. Downhole environment parameters were generated for each month that the well was operational. The measured historical rates were specified as input, and the resulting tubing head pressures were matched to field measured values by tuning the effective permeability in the inflow equations.

In the predictive phase, results from the Arun full-field reservoir simulation study played a crucial role. Reservoir pressure decline, wellstream composition changes, and tubing head pressures were extracted

from the simulation runs. Calculations were carried out into the future for as long as the well would produce above the loading rate. When the well loaded, the tubing size was reduced and calculations were resumed. When the well loaded with a 3.5-inch (8.89 cm) inner diameter tubing string, it was assumed to be permanently shut-in.

Multi-parameter Regression Analysis

The inspection data from the workovers of fourteen Arun wells, which had not been exposed to acid stimulation fluids, provided maximum pit depth data based on measurements of remaining wall thicknesses. The production lives of these fourteen wells ranged from 1.6 to 11.7 years with maximum localized corrosion (pit) penetration rates ranging from 0 to 225 mils per year (mpy) (5.72 mm/y) for the 7-inch (17.78 cm) L80 tubing with a nominal wall thickness of 0.498-inch (1.265 cm). The monthly outputs from the corresponding history phase calculations for each of these wells generated downhole environment parameters for each tubing string segment which included the liquid water and liquid hydrocarbon dropout volumes, liquid film thicknesses and velocities, shear stresses, surface tension, gas and liquid densities and viscosities, superficial gas and liquid velocities, temperatures, and pressures, and individual wellstream components. In addition to the outputs, H_2S and CO_2 concentrations and produced water compositions along with conductivity, total dissolved solids, and pH data were also available from field measurements of test separator samples.

The maximum corrosion penetration rate was used in multi-parameter regression fits against combinations of 65 independent variables to examine the relative influences of the parameters in explaining the variation in the corrosion rates. Polynomial fits were attempted with single variables and combinations of variables. The following quadratic equation expresses a relationship for which the analysis of variance indicated statistical significance:

$$\text{Maximum Penetration Rate (mpy)} = 0.75 + 143.6\,(H_2O/HC) + 430.1\,(H_2O/HC)^2$$

The variable (H_2O/HC) is the volume ratio of liquid water to liquid hydrocarbon on the tubing walls. Figure 2 depicts the relationship graphically. The degree of fit could only be improved marginally with the addition of, or interaction with, other variables. This relationship, while certainly not explaining all of the variability in the corrosion response, suggested that the ratio of liquid water to liquid hydrocarbon was a parameter that had a significant influence on the corrosion behavior of the L80 carbon steel tubing strings in the Arun field.

Natural Corrosion Inhibition by Arun Condensate

Experimental work was then conducted to confirm the degree of natural corrosion inhibition provided by the Arun condensate. Using the reservoir simulation data for field production through the year 2000, critical variable ranges were established to simulate a severe scenario in the future in which the highest acid gas partial pressures would occur within the temperature range from 225 to 275°F (107 to 135 °C). This worst case environment would occur when wellhead pressure and temperature declined to approximately 2000 psi (13790 kPa) and 250°F (121°C), respectively. Corresponding partial pressures for CO_2 and H_2S were established as 300 psi (2069 kPa) and 0.1 psi (0.69 kPa), respectively.

Arun produced water containing 55 ppm chlorides, simulated in the laboratory, and stabilized Arun condensate from the field were used with various L80 carbon steel tubular metallurgies.

Preliminary work was conducted using a flowloop at the University of Aachen, Germany with water to hydrocarbon ratios of 1.0 (50% water: 50% condensate) and 0.25 (20% water: 80% condensate). Localized corrosion, as reflected by a maximum local penetration rate, assuming that a pinhole shaped pit would continue to penetrate the wall thickness of the tubing, was calculated from the pit depth measurements taken using a laser profilometer system. Irrespective of the exact nature of the L80 carbon steel metallurgy tested, both maximum local penetration rate and the general weight loss corrosion rate were significantly reduced as the relative condensate volume was increased. Extensive laboratory work was then conducted to characterize the Arun condensate and evaluate the influence of the water to hydrocarbon ratio on the corrosion behavior under Arun wellbore conditions.

Since the preliminary work had shown that both localized corrosion and general weight loss corrosion had been reduced as the condensate volume increased, an experimental program was designed to quantify the effects of varying the fluid volume ratio, first through the use a short exposure screening test and, subsequently, with longer exposure stirred autoclave tests. The screening tests were conducted under atmospheric pressure at 130°F (54°C) for 10 hours using CO_2 gas with 1000 ppm H_2S in a total liquid volume of 30 ml. The apparatus is depicted in Figure 3. The specimen surface area to water volume ratio was maintained at a minimum of 15 cm.

Autoclave testing was conducted using a fixed cage configuration in one-gallon autoclaves as shown in Figure 4. Exposure time in these tests was 72 hours with the partial pressures and temperature representative of the severe conditions previously referenced. A specimen surface area to liquid water volume ratio of 25 cm was maintained throughout this testing. Unlike previous testing using a high speed rotating cage configuration(2), the cage was fixed and auxiliary propellers were used for stirring. Liquid samples withdrawn from the autoclaves at various depths demonstrated that the propeller configuration and rotation rate significantly influenced the degree of mixing of the water and the condensate fluids. Sufficient mixing to properly expose the steel coupons to the appropriate fluid volume ratio could only be achieved with a fixed cage configuration.

Figure 5 summarizes the influence of water to hydrocarbon ratios on the general weight loss rates and the localized penetration rates from the autoclave tests. At a water to hydrocarbon ratio of 0.25 (20% water, 80% hydrocarbon), the significant inhibiting influence of the Arun condensate is very evident for both localized as well as general corrosion. Realizing that the composition of the condensate would change over time and, in particular, that the higher molecular weight fractions were likely to remain in the reservoir as the pressure diminished, it became important to isolate the range of the inhibiting components and their effectiveness. Molecular characterization of ten representative samples of the Arun condensate over the period from 1979 to 1991 demonstrated that the condensates became slightly depleted in compounds > n-C_{11} and enriched in the lighter hydrocarbon compounds.

A spinning band vacuum distillation unit was then used to separate the Arun condensate into groups of components. The composition of each of the distillation cuts was verified with gas chromatography. Screening tests were conducted to attempt to isolate the range of inhibiting components within the condensate. Figure 6 shows the corrosion responses for the various condensate composition ranges of the distillates at a constant water to hydrocarbon ratio of 14. Clearly, the inhibiting components resided in the component range > n-C_{13} and most likely within the band from n-C_{15} to n-C_{23}. Detailed molecular analysis indicated that the alkylated carbazoles could be responsible for the inhibition. A trend analysis of changes in molecular character with time indicated that the carbazoles in the range of n-C_{17} to n-C_{22} would be expected to remain throughout the flowing life of the reservoir.

Alloy Alternatives

To evaluate other corrosion mitigation opportunities, autoclave testing was also conducted on a variety of 13% chrome alloys, a 15% chrome material, and on 9% chrome-1% molybdenum tubular materials. Table 1 summarizes the test conditions that were used to evaluate the corrosion performance of these materials. No localized corrosion was exhibited by any of the 13% chrome materials or the 15% chrome material tested. The 9% chrome-1% molybdenum materials exhibited slight pitting when exposed to the conditions in test A. Slow strain rate testing of the 13% chrome materials in 300°F (149°C) deoxygenated Arun water at 300 psi (2069 kPa) CO_2 partial pressure and H_2S partial pressures ranging from 0.06 (0.41 kPa) to 0.1 psi (0.69 kPa) with a strain rate of 1x 10 E-6 in. / sec. ($2.5x10^{-5}$ mm/sec.) did not exhibit any evidence of sulfide stress corrosion cracking susceptibility. The 13% chrome alloys were thus viable corrosion mitigation alternatives for the wellbore environmental conditions projected to be prevalent during the remaining flowing life of the Arun wells.

Corrosion Risk Model Development

It is customary when characterizing the localized corrosion response of a material to measure the maximum pit depth from the distribution of pit depths that are visible and use that pit depth and the exposure time to calculate the maximum penetration rate. In a similar fashion, pit depth measurements reported from

workover inspections or caliper logging reflect the maximum pit depths encountered along the lengths of the tubulars.

The classical applications of statistical methods which deal with average values or symmetrical distributions become inadequate when the parameters of interest are the largest or smallest in the range of possible values. The distribution curve of largest values is skewed with the maximum to the left of the mean and exhibits a long tail extending to the right side. This distribution follows mathematical rigor represented by extreme value statistics.[11] Applications for extreme value techniques have included gust velocities for airplanes, extinction times for bacteria, and extremes in meteorological phenomena including floods and droughts. There have also been applications of extreme value statistics to the depths of corrosion pits.[12,13,14]

In using the extreme-value methodology,[15,16,17] all the observed maxima are ranked in order of size from the smallest to the largest. A plotting position is determined for each observation by associating a probability P, where $P = i / (n+1)$ with each observed maximum value (n). The (i) is the rank of the observation, starting with the smallest. When the data are plotted on extreme-value probability paper, an ideal extreme value distribution will plot exactly as a straight line. The closeness of plotted points to a straight line is an indication of how well the data fit the extreme value theory. Figure 7 provides examples of the extreme value fits for two sources of corrosion rate data: pit depths from field workover inspections and pit depths from autoclave testing. The high r^2 values indicate that the extreme value theory is followed relatively well. The degree of fit improves with large data sets and with the use of accurate and reproducible measuring devices.

Using the extreme value fits for field workover, corrosion logging, and laboratory data, a series of extreme value equations with the best fits ($r^2 > .95$) was assembled and plotted collectively. The volume ratio of liquid water to liquid hydrocarbon generated from the tubing hydraulics calculations that corresponded to the exposure time and tubing segment location for each extreme fit line were superimposed on the collective plot. Figure 8 shows the composite plot of the extreme value lines and the water to hydrocarbon ratios. Clearly, the slope of the extreme value line increased as the water to hydrocarbon ratio increased.

Using the extreme value lines, it then became possible to estimate a tubing life expectancy for exposure to the corresponding volume ratios of water to hydrocarbon in the wellbore. Tabulated probability values[15] can be used to calculate the corrosion rate at a 95% probability from the variate, which was the horizontal axis on the extreme value probability paper. When the nominal wall thickness of the tubing, 0.498 inch (1.265 cm), was divided by the corrosion rate at a 95% probability, the life expectancy in years was estimated for the full wall penetration by a corrosion pit.

The estimated life expectancy associated with the volume ratio of liquid water to liquid hydrocarbon to which a portion of the tubing string was exposed constituted the framework of the corrosion risk model. The model is based on probability and is not intended, nor should it be used, to provide quantitative corrosion rate information. It cannot guarantee that corrosion will occur or when it will occur but provides a risk assessment of the potential that it might occur and when it might occur. It can be used as a tool to forecast the influence of corrosion damage on gas deliverability and to evaluate potential scenarios involving investments in corrosion mitigation alternatives.

As shown in Figure 9, as the reservoir pressure drops over time, the volume ratio of liquid water to liquid hydrocarbon increases to large values. However, the wellbore environment conditions are unique for each well and the change in the ratio with time differed for each of the 78 wells. The mean volume of liquid water and the mean volume of liquid hydrocarbon within a tubing segment was calculated from the monthly outputs over two-year producing increments. The ratio of the two means was calculated and the appropriate coefficients from the extreme value equation were selected to represent that time interval. This was repeated for approximately two-year time steps until the production for each well had been terminated.

An iterative computer program was written to use the inputs from the two-year increments to calculate the cumulative pit depths for incremental time steps assuming that once a pit is initiated, it penetrates the tubing wall continuously if the wellbore environment conditions are corrosive. Time increments of less than two years were not used due to evidence of large, non-random variability in the mean fluid volumes. A 95% probability was used to calculate the life expectancy for the full-wall penetration of the tubing using a best

case, a mid-case, and a worst case scenario. The life expectancy was also calculated for smaller increments of wall thickness penetration where the designed structural capacity of the tubing under pressure may have been at risk.

The validity of the model was evaluated using corrosion pit depth data from workover inspections and corrosion logging that had not been used in the development of the model. Figure 10 is a graphical depiction of the correspondence between the risk model predictions for the range of wall thickness and those measured. From this, it was established that there was at least an 80% confidence level for a 95% probability of corrosion risk. This corrosion risk model was then applied to calculate the life expectancies of the carbon steel tubing in each of the tubing segments for each of the 78 wells.

Figure 11 summarizes the comparison of the predicted life expectancy at the uppermost tubing segment of the well vs. the projected flowing life for 18 of the wells. The prediction shows that penetration of the tubing wall will occur due to corrosion in all but a few of the wells prior to the end of their flowing life. In some wells, the tubing penetration would be projected to occur one to two years in advance of a tubing size reduction necessitated by liquid loading conditions in the well. The impact of an earlier-than-expected recompletion to a smaller tubing size on gas deliverability needed to be taken into account in the development of an optimized corrosion management program.

The tubing wall penetration occurs because the natural inhibition protection afforded by the Arun condensate has been diminished by the increasing liquid water volume on the tubing walls. Corrosion mitigation alternatives under consideration included condensate reinjection to adjust the volume ratio of liquid water to liquid hydrocarbon to lower ranges and workovers to replace some or all of the tubing with carbon steel or 13% chrome alloy. Life expectancy calculations were made for each tubing segment in a well, at intervals of 1000 feet or less, in order to evaluate the depth requirement for corrosion mitigation alternatives. The projected depth requirement for the corrosion mitigation varied from well to well but generally averaged approximately the upper-half of the total completion length.

Figure 12 summarizes the life expectancy projections for the uppermost tubing segment after the recompletion of the 18 wells shown in Figure 11 with new L80 carbon steel. In this scenario, the wells were recompleted just prior to the earliest point in time that wall penetration was projected to occur for the original tubing. Of the 18 wells recompleted, half would now be expected to survive until the tubing was changed out and replaced with 5-1/2-inch (14 cm) diameter tubing to maintain the flowing life of the wells.

Corrosion risk model calculations were conducted for a variety of scenarios for each well in order to weigh the impact of the corrosion risk over time on gas deliverability and the cost of the corrosion mitigation option. A corrosion management program emerged from these scenarios that incorporated the most cost-effective combination of the alternatives for the remaining life of the field. The optimized corrosion management program consisted of a combination of the 13% chrome alloy and carbon steel tubing in some wells and the use of carbon steel tubing in others. Corrosion monitoring will continue to provide feedback data for the refinement of the risk model and its application for the cost-effective management of corrosion as the Arun field depletes.

CONCLUSIONS

1. The integration of reservoir simulation data, tubing hydraulics calculations of the downhole wellbore environments, and the corrosion pit distributions from field data and laboratory experiments provided the framework for the development of a corrosion risk model.

2. A multi-parameter regression showed that the volume ratio of liquid water to liquid hydrocarbon on the tubing walls had a significant influence on corrosion behavior in the Arun field.

3. The Arun condensate provided natural corrosion inhibition for carbon steel tubing at a volume ratio of liquid water to liquid hydrocarbon of 0.25.

4. Extreme value methodology provided a good representation of the distribution of corrosion pit depths from field workover inspection, corrosion logging, and laboratory data.

5. A validity analysis of the risk model with a 95% corrosion probability indicated that there was at least an 80% confidence level for the prediction.

6. Life expectancy calculations using the corrosion risk model provided the basis to develop an optimized corrosion management strategy to minimize the impact of corrosion on gas deliverability as the reservoir depletes.

ACKNOWLEDGMENTS

The authors gratefully acknowledge the technical assistance provided by T. Lindsey, C. Walters, C. Hellyer, M. Lawrey, F. Tarzian, and R. Santos in the experimental work conducted at MEPTEC and the contributions of G. Schmitt and W. Bucken at the University of Aachen. The authors also wish to thank Mobil and Pertamina managements for permission to publish this work.

REFERENCES

1. Shea, R. H., Ott, R. E, Salz, L. B.: "Arun Well Simulation Model Development," Corrosion 90, #4, NACE, (April 23-27, 1990).

2. Stegmann, D. W., Hausler, R. H., Cruz, C. I., Sutanto, H.: "Laboratory Studies on Flow Induced Localized Corrosion in CO2/H2S Environments, I. Development of Test Methodology," Corrosion 90, #5, NACE, (April 23-27, 1990).

3. Hausler, R. H., Cruz, C. I., Sutanto, H.: "Laboratory Studies on Flow Induced Localized Corrosion in CO2/H2S Environments, II. Parametric Study on Effect of H2S, Condensate, Metallurgy, and Flowrate," Corrosion 90, #6, NACE, (April 23-27, 1990).

4. Hausler, R. H., Stegmann, D. W., Cruz, C. I., Tjandroso, D.: "Laboratory Studies on Flow Induced Localized Corrosion in CO2/H2S Environments, III. Chemical Corrosion Inhibition," Corrosion 90, #7, NACE, (April 23-27, 1990).

5. Drake, D. E., Sutanto, H., Colwell, J. A., Stiegelmeyer, W. N.: "Corrosion Resistance of Materials Under Arun Field, Indonesia Conditions Part I.," Corrosion 90, #57, NACE, (April 23-27, 1990).

6. Colwell, J. A., Steigelmeyer, W. N., Drake, D. E., Sutanto, H.: "Corrosion Resistance of Materials Under Arun Field, Indonesia Conditions Part II.," Corrosion 90, #58, NACE, (April 23-27, 1990).

7. Sutanto, H., Semerad, V. A. W., Bordelon, T. P.: "Simulation of Future Wellbore Corrosion With Low Production Rate Field Test," Corrosion 91, #571, (March 5-11, 1991).

8. Lotz, U.: "Velocity Effects in Flow Induced Corrosion," Corrosion 90 #27, NACE, (April 23-27, 1990).

9. EnDean, E. J.: "Corrosion Control in the Well Bore," Petr. Engr., (Aug. 1976), p 50.

10. Lotz, U. van Bodegom, L., Ouwehand, C.: "The Effect of Type of Oil or Gas Condensate on Carbonic Acid Corrosion," Corrosion 90 #41, NACE, (April 23-27, 1990).

11. Gumbel, E. J.: *Statistics of Extremes*, Columbia University Press, New York City, (1958), p 20.

12. Aziz, P. M.: "Application of the Statistical Theory of Extreme Values to the Analysis of Maximum Pit Depth Data for Aluminum," Corrosion, vol. 12, (Oct. 1956), p 495t.

13. Eldredge, G. G.: "Analysis of Corrosion Pitting by Extreme-Value Statistics and Its Application to Oil Well Tubing Caliper Surveys," Corrosion, vol. 13, (Jan. 1957), p 51t.

14. Nicholls, J. R., Stephenson, D. J.: "A Life Prediction Model for Coatings Based On The Statistical Analysis of Hot Salt Corrosion Performance," Corrosion Science, vol. 33, no. 8, (1992), p 1313.

15. Probability Tables for the Analysis of Extreme-Value Data, National Bureau of Standards, Applied Mathematics Series 22, (July 6, 1953), U.S. Dept. of Commerce.

16. Natrella, M. G.: *Experimental Statistics,* National Bureau of Standards Handbook 91, (August 1963), U.S. Dept. of Commerce, p 19-1.

17. Hahn, G. J., Shapiro, S. S.: Statistical *Models in Engineering,* John Wiley & Sons, New York City, (1967), p 112.

18. Peng, D. Y. and Robinson, D. B., "A New Two-Constant Equation of State," I. & E.C. Fundamentals, Vol. 15, no. 1, (1976), p 59.

19. API Manual 14BM: SSCSV Sizing Computer Program, 2nd Edition, Appendix B - Vertical Flow Correlation - Gas Wells, (1978), p 38.

TABLE 1
AUTOCLAVE CONDITIONS USED TO EVALUATE CHROME ALLOYS

Test	Environment	Temperature (°F)	ExposureTime (hrs.)
A.	Air saturated Arun simulated water, 300 psi CO_2, 0.1 psi H_2S partial pressure	250	72
B.	Test A conditions but with non-deoxygenated Arun simulated water	250	72
C.	Test A conditions but with deoxygenated Arun simulated water	250	72
D.	Test A conditions but with deoxygenated Arun simulated water	300	72
E.	Test A conditions but with deoxygenated Arun simulated water	350	72
F.	Deoxygenated Arun simulated water and Arun condensate at a volume ratio of 4, with 300 psi CO_2, 0.1 psi H_2S partial pressure	250	72
G.	Test F conditions but with a volume ratio of 14	250	72

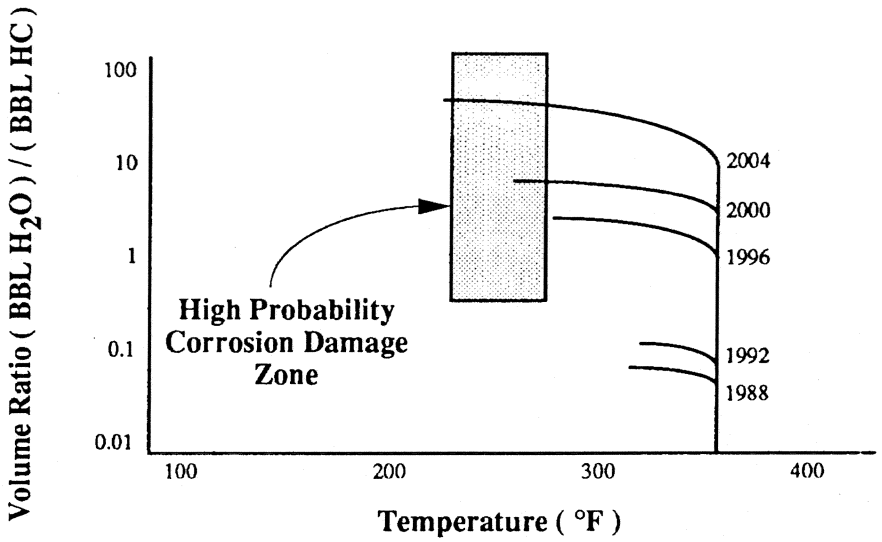

Figure 1. **Fluid volume ratio profiles from the bottom to the top of the tubing string in one Arun well throughout time. The boundaries of the high probability corrosion damage zone are superimposed. The bottomhole temperature is approximately 325°F (178°C) throughout time. (1 mpy=0.0254 mm/yr)**

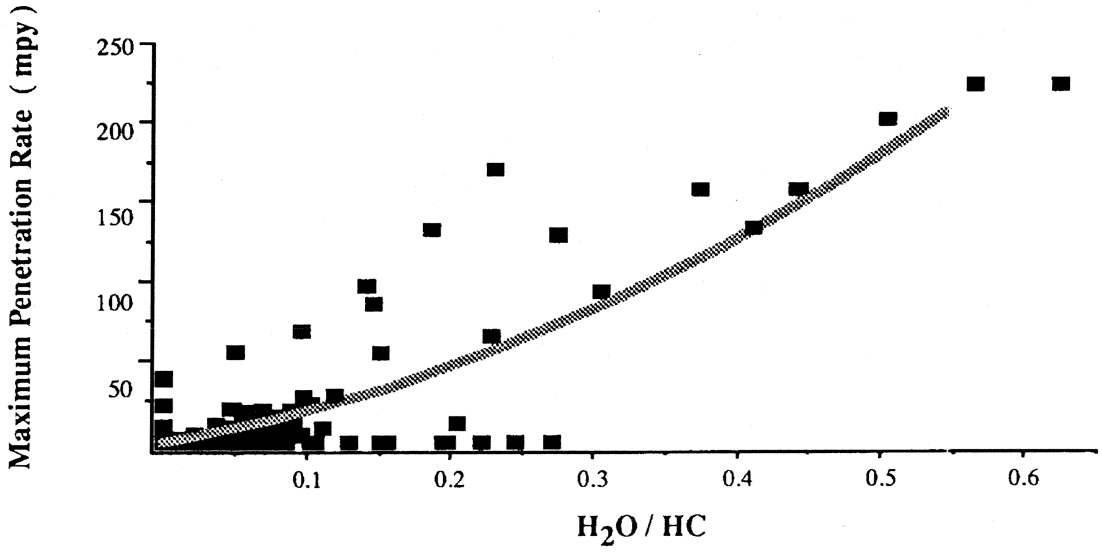

Figure 2. **The quadratic fit for the volume ratio of liquid water to liquid hydrocarbon on the tubing walls vs. the maximum corrosion penetration rate in mils per year. The r^2 correlation coefficient for the fit was 0.749. (1 mpy = 0.0254 mm/yr)**

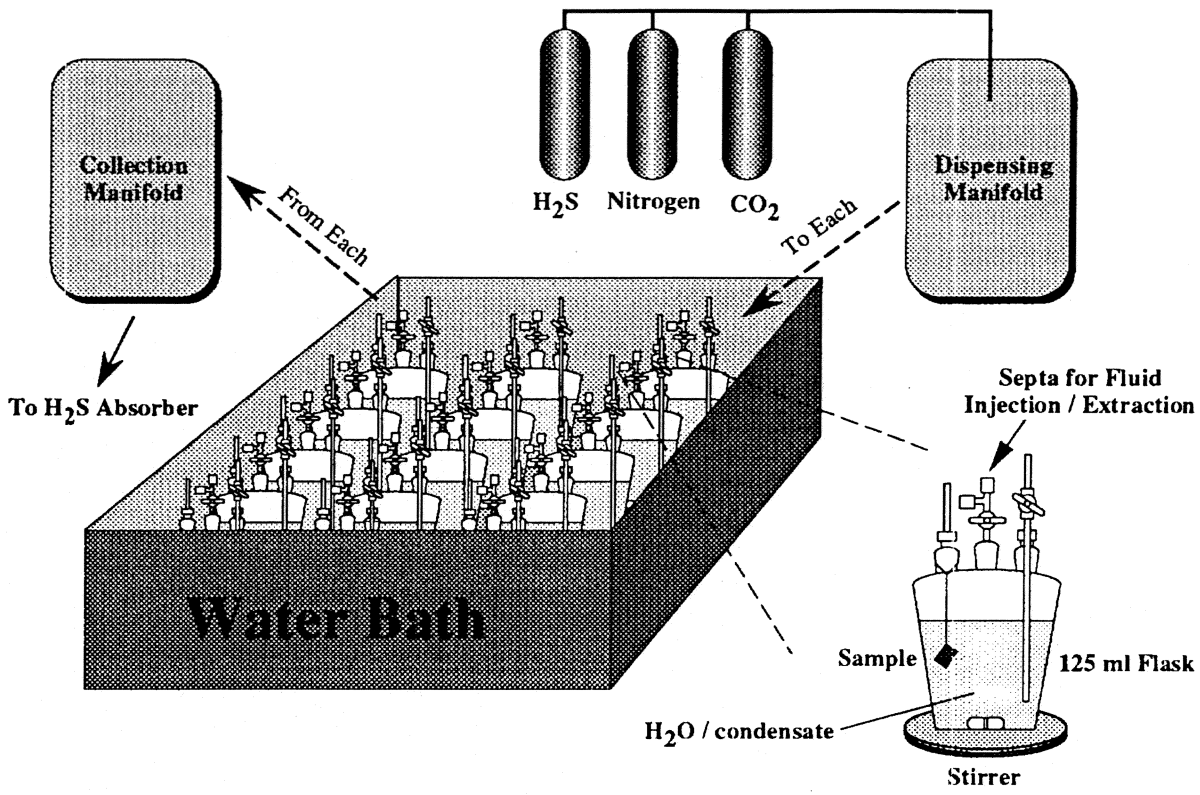

Figure 3. Atmospheric Screening Test Apparatus

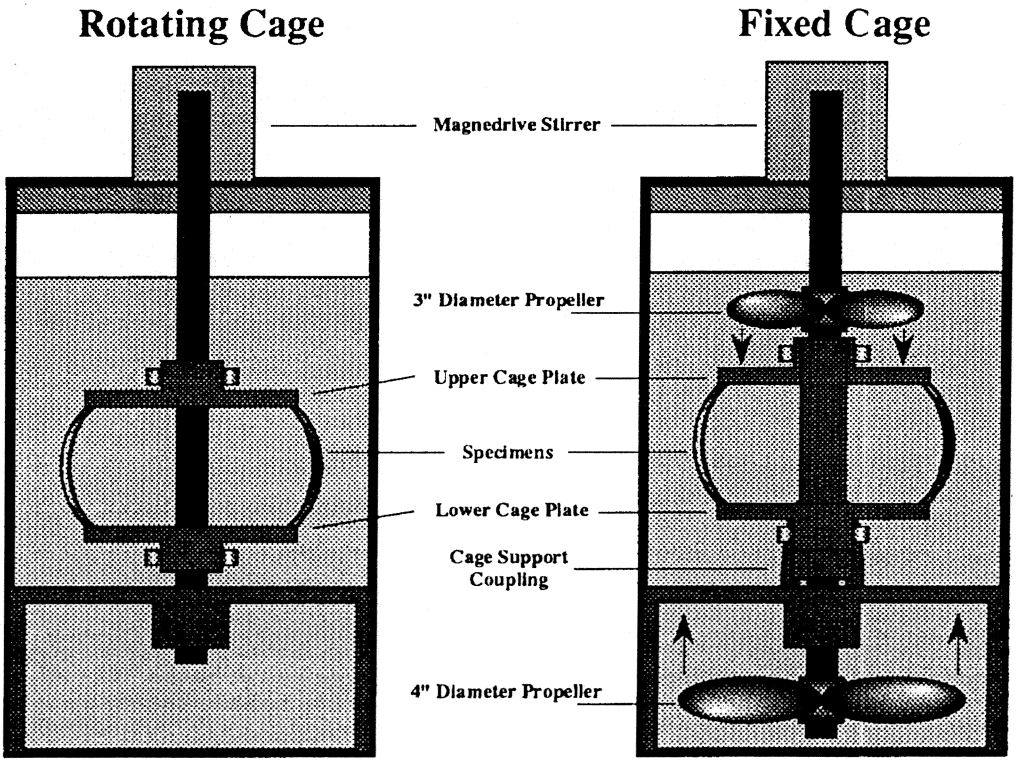

Figure 4. Comparison of autoclave test configurations for a rotating cage and a fixed cage. (1 inch = 2.54 cm)

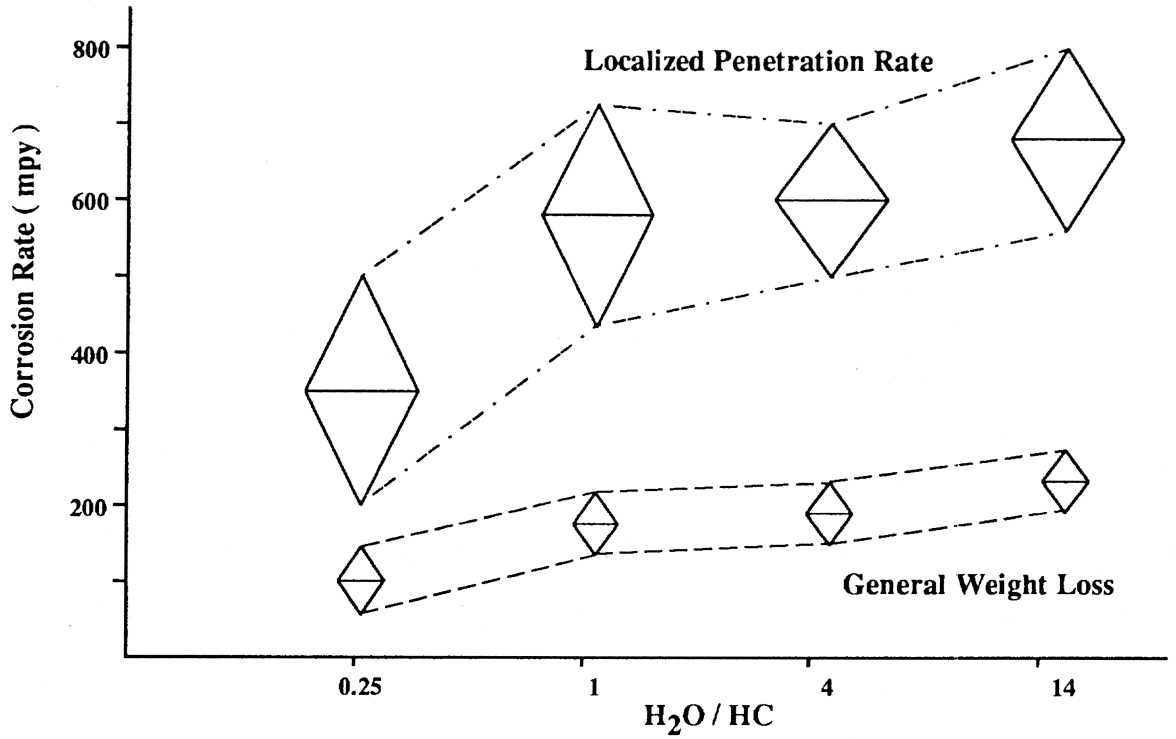

Figure 5. **Influence of volume ratio of liquid water to liquid hydrocarbon on general weight loss corrosion rates and on maximum localized penetration rates from autoclave tests. The size of the diamond represents the 95% confidence about the mean, shown as the horizontal line. (1 mpy = 0.0254 mm/yr)**

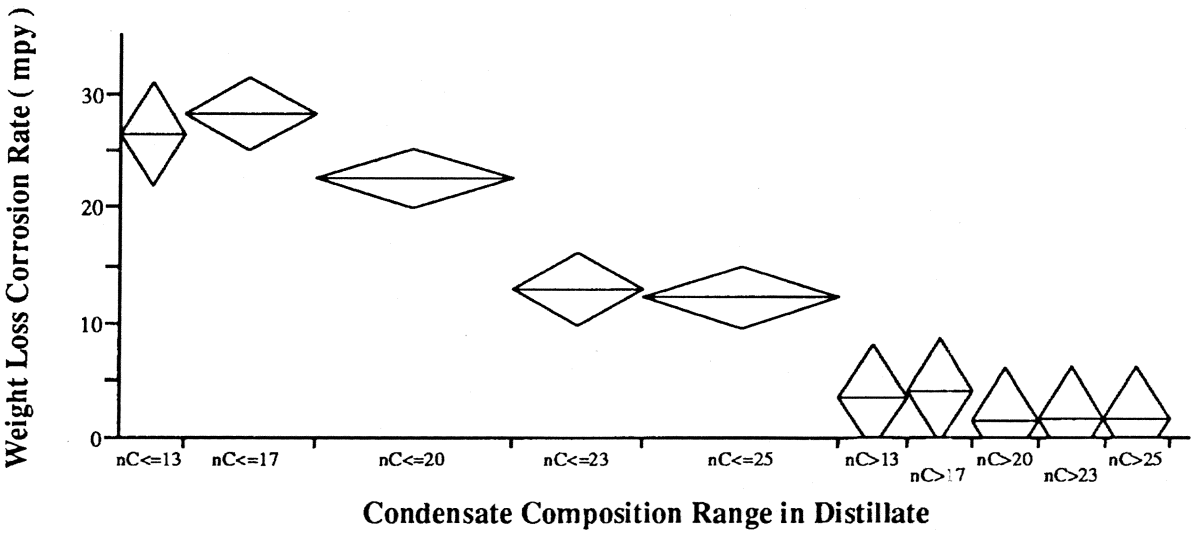

Figure 6. **Weight loss corrosion rates for the compositional ranges in the condensate distillates as determined by the screening test at a constant volume ratio of liquid water to liquid condensate distillate fraction of 14. (1 mpy = 0.0254 mm/yr)**

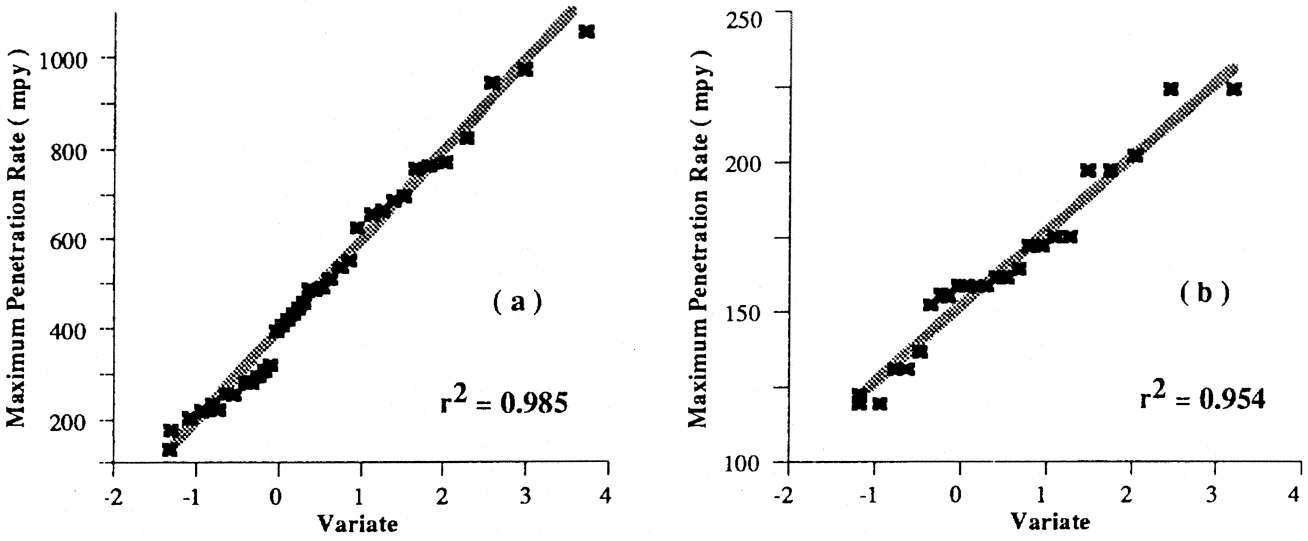

Figure 7. **Extreme value plots for laboratory autoclave tests with Arun saturated water only (a) and for field workover data from a well (b). (1 mpy = 0.0254 mm/yr)**

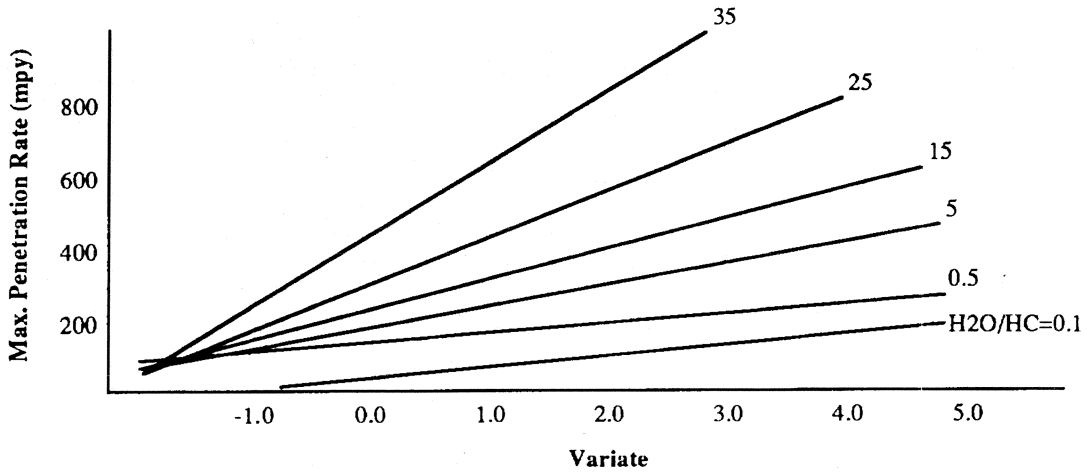

Figure 8. **Composite plot of extreme value fits for both field and laboratory data and corresponding volume ratios of liquid water to liquid hydrocarbon. (1 mpy = 0.0254 mm/yr)**

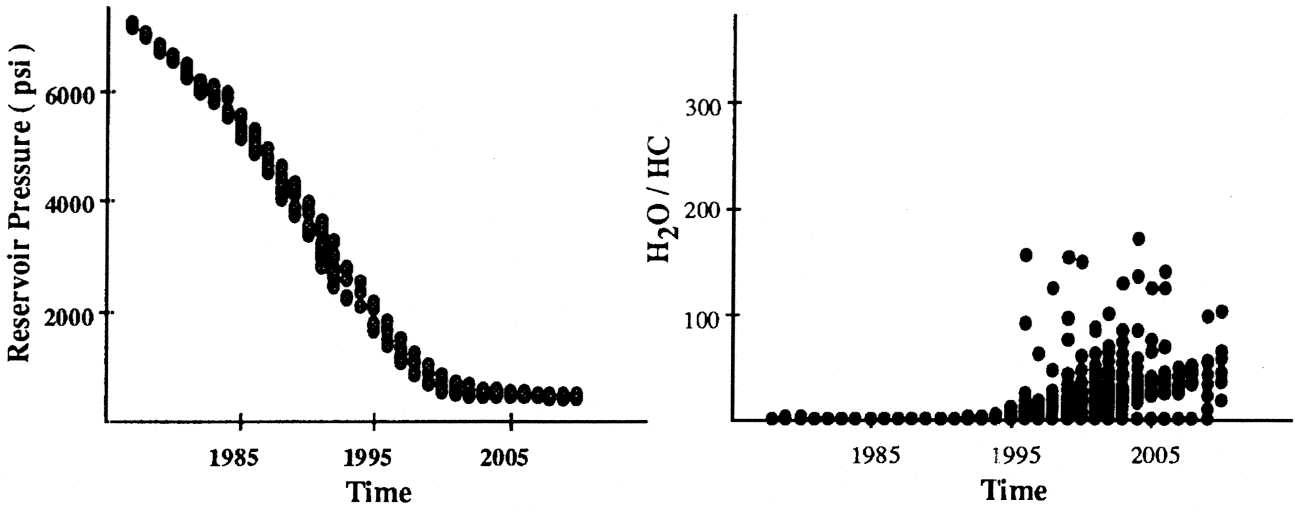

Figure 9. **Changes in reservoir pressure and the volume ratio of liquid water to liquid hydrocarbon over time from reservoir simulation and the tubing hydraulics calculations. (1 psi = 6.895 kPa)**

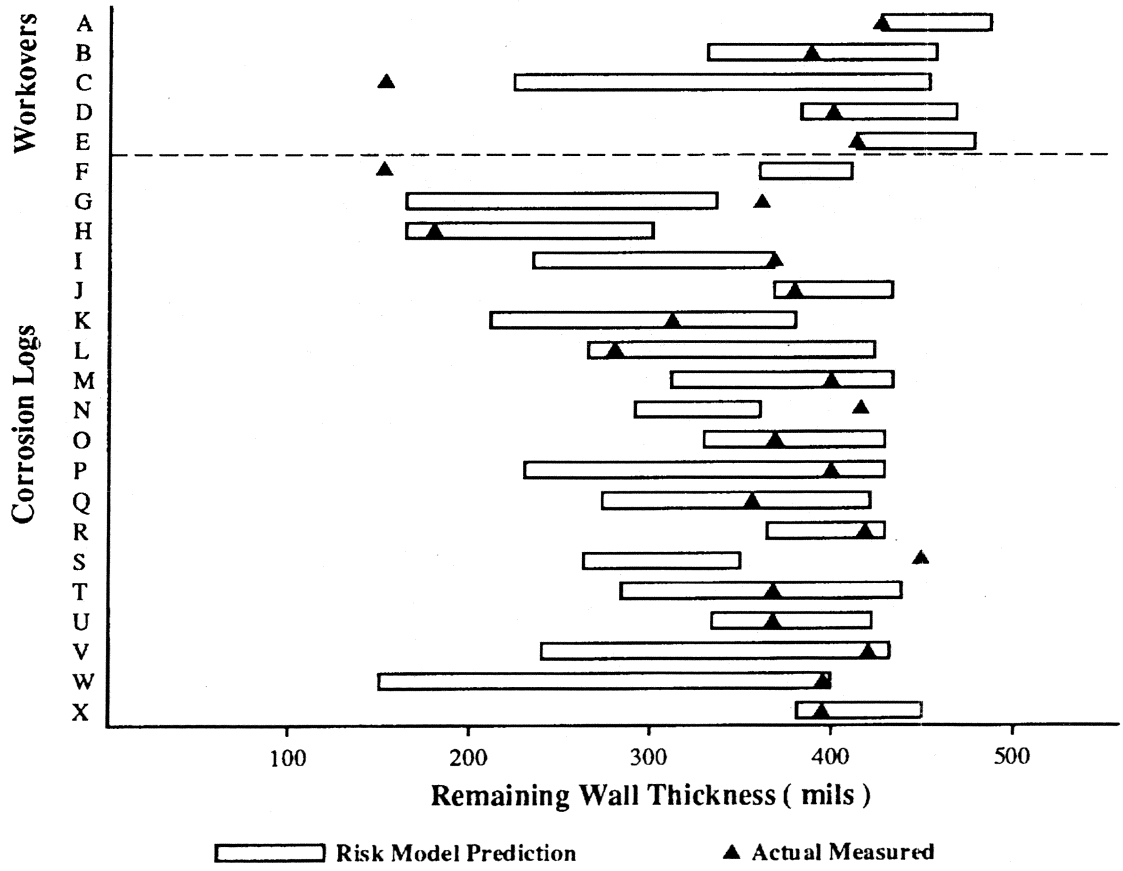

Figure 10. **Summary of validity check for corrosion risk model with workover and corrosion logging data. (1 mil = 0.0254 mm)**

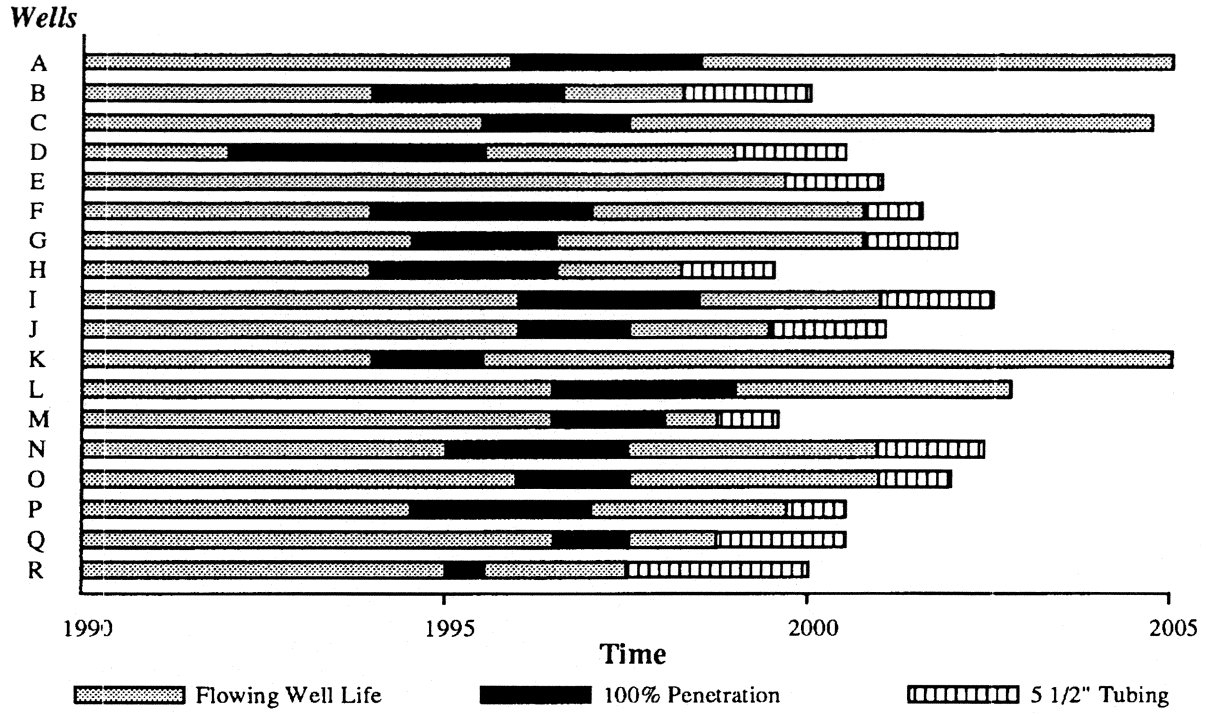

Figure 11. **Summary of the life expectancies for the uppermost segment of carbon steel strings in 18 Arun wells based on the corrosion risk model estimates. A comparison is made with the flowing well life and the projected timing for recompletion with 5 1/2" (14 cm) tubing is shown.**

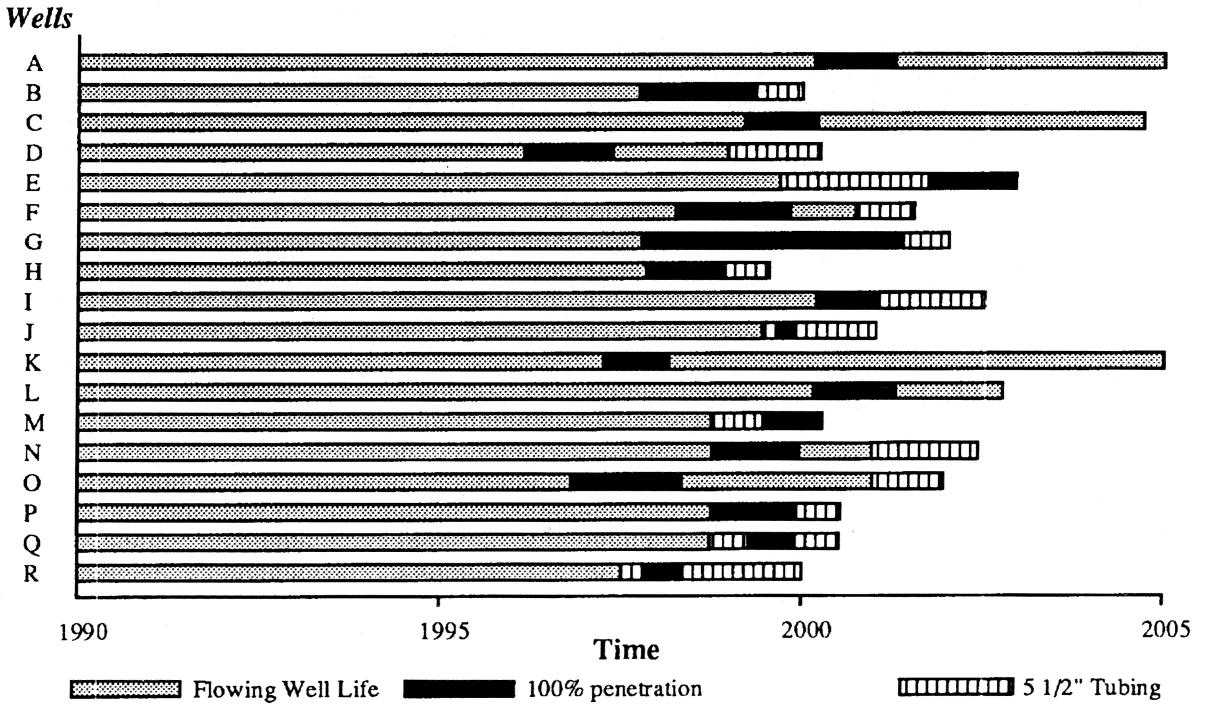

Figure 12. **Summary of the life expectancies for the uppermost segment of carbon steel tubing strings in the same 18 Arun wells in *Figure 11*, for which recompletion was made with new carbon steel prior to the onset of wall penetration of the original tubing. (5 1/2" = 14 cm)**